Vision Research 122 (2016) 93–104

Contents lists available at ScienceDirect

Vision Research

journal homepage: www.elsevier.com/locate/visres

Eye movements between saccades: Measuring ocular drift and tremor

Hee-kyoung Ko [a], D. Max Snodderly [a], Martina Poletti [b,*]

[a] Department of Neuroscience, Institute for Neuroscience, and Center for Perceptual Systems, University of Texas at Austin, United States
[b] Department of Psychological and Brain Sciences, Boston University, Boston, MA 02215, United States

ARTICLE INFO

Article history:
Received 10 May 2015
Received in revised form 17 March 2016
Accepted 17 March 2016
Available online 17 April 2016

Keywords:
Eye coil
Dual Purkinje Image eyetracker
Ocular tremor
Ocular drift
Intersaccadic retinal motion
Fixational eye movements

ABSTRACT

Intersaccadic periods of fixation are characterized by incessant retinal motion due to small eye movements. While these movements are often disregarded as noise, the temporal modulations they introduce to retinal receptors are significant. However, analysis of these input modulations is challenging because the intersaccadic eye motion is close to the resolution limits of most eyetrackers, including widespread pupil-based video systems. Here, we analyzed in depth the limits of two high-precision eyetrackers, the Dual-Purkinje Image and the scleral search coil, and compared the intersaccadic eye movements of humans to those of a non-human primate. By means of a model eye we determined that the resolution of both techniques is sufficient to reliably measure intersaccadic ocular activity up to approximately 80 Hz. Our results show that the characteristics of ocular drift are remarkably similar in the two species; a clear deviation from a scale-invariant spectrum occurs in the range between 50 and 100 Hz, generally attributed to ocular tremor, leading to intersaccadic retinal speeds as high as 1.5 deg/s. The amplitude of this deviation differs on the two axes of motion. In addition to our experimental observations, we suggest basic guidelines to evaluate the performance of eyetrackers and to optimize experimental conditions for the measurement of ocular drift and tremor.

1. Introduction

As we scan a visual scene, rapid eye movements, known as saccades, alternate with periods of fixation. Most visual information –especially the fine detail of images– is acquired during these fixational pauses. However, the term "fixation" is misleading, because the eye is never completely stationary. In addition to occasional microsaccades, incessant eye drifts and a small high-frequency perturbation, known as tremor, continually occur during these periods (Collewijn & Kowler, 2008). Intersaccadic eye movements shift the retinal image by considerable amounts (over an area as large as 1 deg^2), yet vision research studies rarely consider them. For example, neural responses are often studied as if the eyes were stationary during fixation (*e.g.* Vinje & Gallant (2000) and Haslinger et al. (2012)). In fact, fixational eye movements are commonly regarded as a nuisance because they are not under the control of the experimenter.

Despite the little attention from the vision research community, intersaccadic eye movements appear important for the acquisition and subsequent processing of the visual signal (Ahissar & Arieli, 2012; Arend, 1973; Averill & Weymouth, 1925; Aytekin, Victor, & Rucci, 2014; Desbordes & Rucci, 2007; Kuang, Poletti, Victor, & Rucci, 2012; Marshall & Talbot, 1942; Rucci & Casile, 2004; Rucci, Iovin, Poletti, & Santini, 2007; Rucci & Victor, 2015; Steinman & Collewijn, 1980). Moreover, many V1 neurons exhibit maintained firing during these movements, presumably contributing to perception of fine detail (Kagan, Gur, & Snodderly, 2008; Snodderly, Kagan, & Gur, 2001; Snodderly, 2016). Characterizing the spatiotemporal input during intersaccadic periods is, therefore, essential for a better understanding of visual mechanisms.

Ocular drift has been studied primarily in humans (Cherici, Kuang, Poletti, & Rucci, 2012; Ditchburn, 1973; Engbert & Kliegl, 2004; Fiorentini & Ercoles, 1966; Krauskopf, Cornsweet, & Riggs, 1960; Kuang et al., 2012; Nachmias, 1961; Nachmias, 1959; Rattle, 1969; Steinman, 1965; Skavenski & Steinman, 1970; Steinman, Haddad, Skavenski, & Wyman, 1973; Sansbury, Skavenski, Haddad, & Steinman, 1973; Rucci et al., 2007). It has often been described as a random walk (Burak, Rokni, Meister, & Sompolinsky, 2010; Kuang et al., 2012), or a self-avoiding random walk (Engbert, Mergenthaler, Sinn, & Pikovsky, 2011) that has extremely low speed ($< 10'/s$) (Ditchburn, 1973) and to displaces the eye by very small amounts (Nachmias, 1961; Steinman, 1965). However, because of technical limitations, older studies could only measure the average displacements over a relatively large interval, typically the entire intersaccadic period. This

* Corresponding author.
E-mail address: martinap@bu.edu (M. Poletti).

http://dx.doi.org/10.1016/j.visres.2016.03.006
0042-6989/

approach models ocular drift as uniform linear motion and neglects its curvilinear component, resulting in a serious underestimation of its instantaneous velocity. More recent work has reported the mean instantaneous speed of ocular drift to be approximately 50′/s (Cherici et al., 2012; Rucci & Poletti, 2015).

Even fewer studies have focused on ocular tremor (Bolger, Bojanic, Sheahan, Coakley, & Malone, 1999; Coakley, 1983; Eizenman, Hallett, & Frecker, 1985; Spauschus, Marsden, Halliday, Rosenberg, & Brown, 1999), to the point that its very existence as a genuine oculomotor signal has been debated. While some studies have observed a deviation from the drift spectrum in the 50–100 Hz range (Eizenman et al., 1985; Spauschus et al., 1999), more recent research did not find any clear spectral deviation in this frequency band (Sheehy et al., 2012; Stevenson, Roorda, & Kumar, 2010). However, these studies differ in multiple ways beyond the recording techniques, including the method for spectral estimation and the duration of the intersaccadic periods analyzed. These procedural differences may affect the estimation of spectral density, and further analyses seem warranted.

One of the reasons why intersaccadic eye movements are often ignored is because measuring drift and tremor with high precision and accuracy is challenging. These movements appear to be beyond the resolution of the most popular video eyetrackers currently available (*e.g.*, Eyelink 2000), and the application of video eyetrackers to the study of drift and tremor is problematic for a number of reasons (Drewes, Zhu, Hu, & Hu, 2014; Kimmel, Mammo, & Newsome, 2012). First, current pupil-based eyetrackers suffer from slow artifactual drifts related to the decentration of the pupil (Bedell & Stevenson, 2013; Choe, Blake, & Lee, 2016; Drewes, Masson, & Montagnini, 2012; Drewes et al., 2014; Merchant, Morrissette, & Porterfield, 1974; Wildenmann & Schaeffel, 2013), which can be easily mistaken for ocular drift. Second, various factors, such as the color of the iris, the presence of visual aids, the specific calibration methods used, lack of proper head immobilization and/or slippage of the head mounted eyetracker, together contribute to reduce the precision of measurements (Houben, Goumans, & van der Steen, 2006; Kolakowski & Pelz, 2006; Nystrom, Andersson, Holmqvist, & van de Weijer, 2013). Furthermore, these systems perform undisclosed internal filtering operations that are not under the experimenter's control (Holmqvist et al., 2011), and realistic assessments of sensitivity with model eyes have not been performed.

Given the current limitations of video eyetrackers, much of what we know about intersaccadic fixational movements comes from other techniques. Two methods have primarily been used: the Dual-Purkinje Image eyetracker (Crane & Steele, 1985) and the scleral search coil (Robinson, 1963). But what are the limits of these methods? Can they reliably record drift and ocular tremor? To address these questions, we made measurements of gain, noise, and slow instrumental drift in both systems. Furthermore, we compared the characteristics of intersaccadic eye movements in humans to those of the macaque monkey. Our measurements show that both systems are capable of recording extremely small eye movements. More broadly, the general approach described here can be used as a guideline to document the precision of different eyetracking systems and their capability to characterize intersaccadic motion.

2. Methods

We first assessed the capabilities of the eye coil and the DPI system to reliably measure intersaccadic motion using a model eye and a test coil that can mimic the signal from a real eye, then we examined the temporal characteristics of intersaccadic eye movements in humans and in a non-human primate.

2.1. DPI eyetracker

Apparatus. A DPI eyetracker (v.6, Fourward Technology) was employed. This system uses the first and the fourth Purkinje reflections from optical surfaces in the anterior segment of the eye. The first-Purkinje image is generated by reflection of a collimated infrared (IR) light from the front surface of the cornea, while the fourth-Purkinje image is generated by the IR reflection from the rear surface of the ocular lens. The output of the eyetracker is based on the relative distance between the two Purkinje images. The spatial separation of the images varies with eye rotation and can be measured accurately with a resolution of 1 arcmin (Crane & Steele, 1985). If the eye undergoes translation, both reflections move the same amount in the same direction. On the other hand, when the eye rotates, the separation between the two reflections changes. Therefore the eyetracker output is minimally affected by small translations of the head (Crane & Steele, 1978). Vertical and horizontal eye positions were sampled at 1 kHz, and recorded for subsequent analysis by means of a custom-made system for gaze contingent control (EyeRIS) (Santini, Redner, Iovin, & Rucci, 2007).

Procedure. The precision, resolution, long-term drift and temporal characterization of the noise of the DPI were assessed by using a model eye. The model eye consisted of a pair of lenses mimicking the IR reflections from the lenses of a human eye that could be tracked in the same manner as a real eye. The measurements with the model eye were conducted with the light intensity levels of the Purkinje images adjusted to values that are representative of values for human subjects. Note that the model eye does not fully replicate all the characteristics of a biological eye. In particular some sources of noise present in the biological eye might not be reproduced when using a model eye. Whilst imperfect, the model eye can provide an essential estimate of the lower bound of the system noise.

The precision of the DPI eyetracker is mostly determined by the CCD sensor noise, and by the mechanical components of the servo motors. Quantization noise in the analog to digital conversion and recording of the output is negligible. The noise and drift of the DPI eyetracker was assessed by means of a stationary model eye (Fig. 1A) locked in the straight-ahead direction; each recording lasted 10 s ($N = 36$). Log-term drift in the noise was assessed with recordings of 10 min duration ($N = 6$).

Resolution of the DPI eyetracker was estimated with controlled rotations of the model eye mounted on a calibrated galvanometer (CX-600, General Scanning Inc.). The galvanometer had one degree of freedom and moved the eye diagonally.

Assessment of the temporal characterization of human intersaccadic periods was based on a dataset collected from four naïve emmetropic human subjects during sustained fixation on a blank screen in a dimly illuminated room; subjects were instructed to maintain their gaze in the central region of the display. Subjects' heads were immobilized by means of head-rests and a dental imprint bite bar. Informed consent was obtained from all participants following the procedures approved by the Boston University Charles River Campus Institutional Review Board. Data from all subjects have been pooled together. Results did not change when data were averaged across subjects.

Data analysis. Human eye movement recordings were segmented into intersaccadic periods based on eye velocity. Movements with speeds larger than 3 deg/s and amplitudes exceeding 3 arcmin were classified as saccades. Identification of intersaccadic periods was performed automatically and then validated by human experts. To avoid lens wobble artifacts (Deubel & Bridgeman, 1995a, 1995b; Stevenson & Roorda, 2005) our custom algorithm for saccade and microsaccade detection merged consecutive events closer than 15 ms into a single saccade, automatically excluding post and pre-saccadic overshoots from the adjacent drift periods.

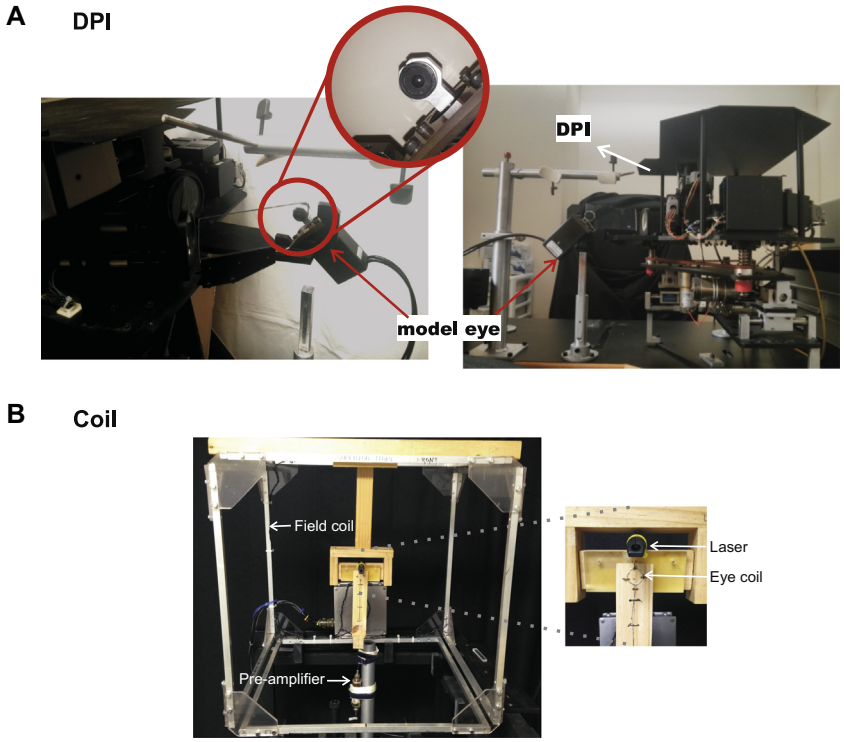

Fig. 1. Experimental setups used to measure the eyetrackers' precision. (A) A model eye mimicking the first and the fourth Purkinje reflections from a human eye was mounted on a static stage or on a calibrated galvanometer (as shown in the figure). The galvanometer was driven by a function generator and was used to measure the DPI resolution. (B) A test search coil with the same characteristics as one implanted on the eye of a monkey was mounted with thread on a wooden shim. The eye coil was clamped in the straight-ahead position at the center of the field coil to record the voltages generated by noise and drift. To measure the gain of the system the coil was rotated with an attached laser pointer aimed at the stimulus monitor and the voltage output per arcmin of rotation was calculated by trigonometry.

Peri-saccadic and peri-microsaccadic periods were removed by discarding the initial and the final 50 ms of the selected intersaccadic segments, limiting the analysis to periods of steady fixation during which the speed of eye movements remained constant.

We examined the temporal characteristics of both intersaccadic periods and system noise. To achieve a reliable estimate of the intersaccadic power spectrum we used the Welch method (Welch, 1967). This method consists of dividing the time series data into overlapping segments, computing a modified periodogram of each segment, and then averaging across the segment estimates. The redundancies introduced by overlapping between segments were reduced by the use of a nonrectangular (Hanning) window. The sample size of this window determines the resolution of the spectrum; larger sizes allow for higher resolution. Preferably, for the 50% overlap used here, the size of the window should be at least half the size of the data samples. Therefore, the length of intersaccadic periods is a crucial factor, and because fixations are relatively short (generally less than 500 ms, due to frequent microsaccadic interruptions; for the dataset used here the average duration of intersaccadic periods was 384 ± 1251 ms) it often represents a limitation in the spectral resolution that can be achieved.

In order to maximize the power spectrum resolution we selected only intersaccadic periods longer than 3 s, and we used a window of 1024 samples (results displayed in Fig. 5A). This allowed us to resolve frequencies ranging from 1 to 500 Hz. Based on this criterion we selected a total of 500 intersaccadic segments. Note that for the coil recordings, because intersaccadic periods longer than 500 ms were very rare for the tested monkey, the power spectrum estimate has a lower resolution. Therefore, to directly compare intersaccadic temporal characteristics of human and non-human primates in Fig. 6 the spectrum for the data collected with the DPI was based on segments of size comparable to those selected for the coil, using a window of 256 samples.

We used the raw unfiltered data for the computation of the power spectrum. Based on the comparison between the power spectrum of noise and that of intersaccadic motion we determined the temporal frequency up to which the DPI and the eye coil system can reliably measure intersaccadic motion. This frequency was then used as the cut-off frequency to low-pass filter the eye movement signal with a Savitzky-Golay filter, which can smooth out the signal with minimal distortion of its original properties (Awal, Mostafa, & Ahmad, 2011; Gorry, 1990). Computations of intersaccadic speed were based on the filtered data.

2.2. Eye-coil system

Apparatus. Performance of the eye coil system (eye-coil, Remmel Labs, model EM7) was characterized with the aid of a test coil as illustrated in Fig. 1B. A search coil was fabricated from Teflon-insulated stainless steel wire, with 3 turns forming a coil 14 mm in diameter continuous with twisted leads terminating in connector pins mating with a shielded cable. The coil was formed from slightly thicker wire (Cooner Wire, AS634) than that used in many laboratories, which results in greater durability and lower resistance. The low coil resistance (19.5 ohms for the test coil) may contribute to the low noise values that we obtain. The structure of the test coil was identical to that of a coil implanted under the conjunctiva of the eye of a rhesus monkey (Judge, Richmond, & Chu, 1980). The implanted coil was securely sutured to the sclera. In our experience (DMS) coils attached with cyanoacrylate tissue glues can come loose over time and slip on the sclera. All procedures in the animal experiments conformed to the National Institutes of Health (NIH) guidelines and were approved by the Institutional Animal Care and Use Committee of the University of Texas at Austin.

The measurements reported here were performed with a Remmel labs EM7 eye movement monitor (Remmel, 1984), which

has a preamplifier (gain ≈40×) placed near the eye coil and a main amplifier and control box connected to the preamplifier by a long cable. The test coil was mounted on a tapered wooden strip (a carpenter's shim) with silk thread. The leads from the eye coil were oriented vertically along the long axis of the strip before connecting to a shielded cable to the preamplifier, which was encased in a copper pipe. The cable to the preamplifier and the cable from the preamplifier to the main control box were RG58/U coaxial cables, which were chosen because their diameter is sufficient to minimize noise pickup and to avoid spurious induced voltages. The same preamplifier and cables were used in experiments with the monkey.

The coil was either clamped in the straight-ahead position to measure noise and drift or the coil was rotated over a range of ±5° to estimate the gain of the eye movement monitor as voltage output per arcmin rotation. A laser pointer rigidly attached to the coil mount was aimed at the stimulus screen to indicate the orientation of the coil. Signals from the coil were sampled with a custom-made system for gaze contingent control (EyeRIS) at 1000 Hz (Santini et al., 2007).

To characterize the system in a state appropriate for recording the smallest eye movements, we adjusted the controls to about 80% of the maximum gain of the EM7 system. This results in a maximum range of at least ±20°, which is sufficient to accommodate a large variety of behavioral tasks. It is also possible to adjust the system for lower sensitivity and larger range if the task requires it.

Procedure. The output of the EM7 was sampled while the laser and the eye coil were aimed at a square calibration grid of 9 points for 1 s at each location; this procedure was repeated 3–5 times. Mean output at each of the angular positions was calculated to obtain an initial estimate of the gain of the system. The true value of the gain in actual practice was determined by having the monkey repeatedly fixate for 2 s at the same locations on the display that were used for the test coil recordings. Median values of the signals from the monkey's eye coil at each fixation location were calculated to estimate the true gain. The estimates from the test coil data and from the monkey data agreed within experimental error.

The noise of the system was calculated based on recordings acquired while the coil was clamped in the straight-ahead position. Root-mean-square values of the output were calculated for each minute of recording and averaged to derive a measure of the noise, based on 360 recordings, each of 5 s duration. Long-term drifts were measured over 6 recordings of 10 min each. An average measure of the drift amplitude was then calculated over 6 recordings.

Data analysis. Similar to the analyses of the DPI eyetracker signals, the power spectrum of the noise and of the monkey's intersaccadic periods was calculated by means of the Welch method with 50% block overlap (window length: 256 ms), however, for the monkey, shorter intersaccadic epochs were included ($N = 490$, minimum duration 385 ms, average duration of intersaccadic periods: 552 ± 163 ms). For the power spectrum of the noise with the test coil, 10 samples of 3 min duration were used. For the power spectrum of the monkey's intersaccadic intervals, data were collected on four different days as described in the results.

3. Results

3.1. Data quality assessment

The results of the noise measurements are illustrated in Figs. 2 and 3, and numerical data are summarized in Table 1.

DPI system. The noise was characterized by recording the signal generated by the system when the model eye was mounted on a stationary stage (Fig. 1A). Recordings were periodically carried out over the course of a year. According to a previous assessment performed by Crane and Steele (Crane & Steele, 1985), the noise

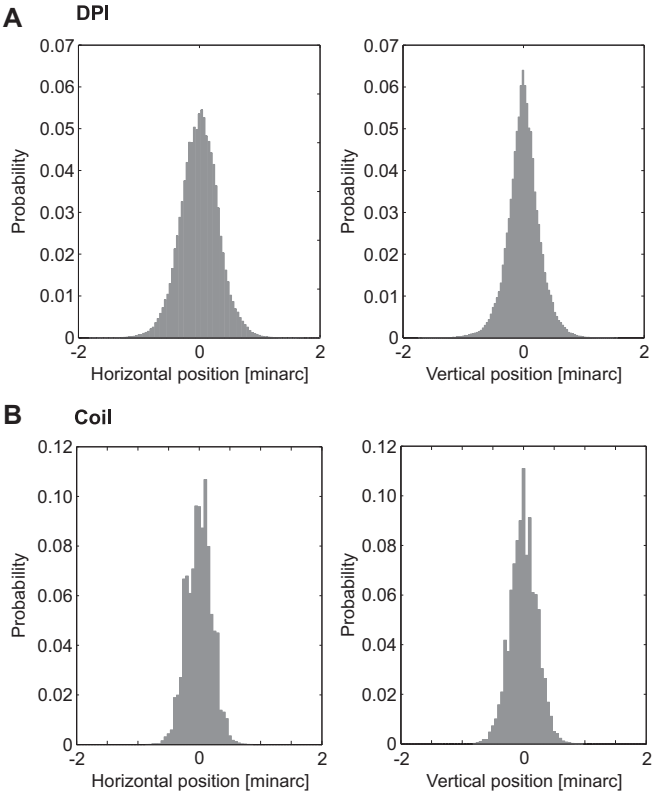

Fig. 2. Noise distributions of the eyetrackers. (A) DPI eyetracker. (B) Eye coil. The eyetracker signal was sampled at 1 kHz while tracking a stationary model eye (DPI) or eye coil. Histograms represent instantaneous position values on the horizontal and the vertical axes. Mean position was subtracted from each recording. Distributions are based on 36 recordings of 10 s duration each collected over a period of several months for the DPI eyetracker and on 360 recordings of 5 s duration each for the eye coil.

of the DPI eyetracker has a RMS of 20 arcsec (0.333 arcmin). As illustrated in Table 1 and in Fig. 2A our measurements show a similar level of noise.

However, measuring the noise over such short, 10 s, periods does not reveal the potential presence of slow drifts in the signal, which can have a negative impact on the accuracy and precision of the eyetracker. Therefore, to measure these slow drifts, the signal from the static model eye was recorded over a 10 min period, based on the consideration that a session of data collection with human subjects does not usually last longer than 10 min.

As the slow drift was consistently unidirectional, the total displacement it produced was calculated as the Euclidean distance between the average position over the first and last second of the recording. Fig. 3 shows an example of one recording; on average, over 10 min, the slow drift covered a distance of $0.7 \pm 0.29'$ ($N = 6$), and it was more pronounced on the vertical axis ($0.62' \pm 0.32'$) than on the horizontal axis ($0.27' \pm 0.12'$).

The impact of this slow drift on the quality of the recordings is negligible for most purposes as it produces a net displacement of less than 1 arcmin over 10 min. Moreover, with human subjects, to maintain the accuracy of gaze localization throughout a recording session, the eye movement signal is adjusted by frequently re-computing, by means of gaze-contingent techniques, the offset between the estimated center of gaze and the actual line of sight (Poletti & Rucci, 2016).

While measuring the noise of an eyetracker provides an estimate of its precision, it does not specify its resolution, that is, the smallest gaze shift that can be reliably detected. For this purpose, we examined the output from the DPI when controlling the motion

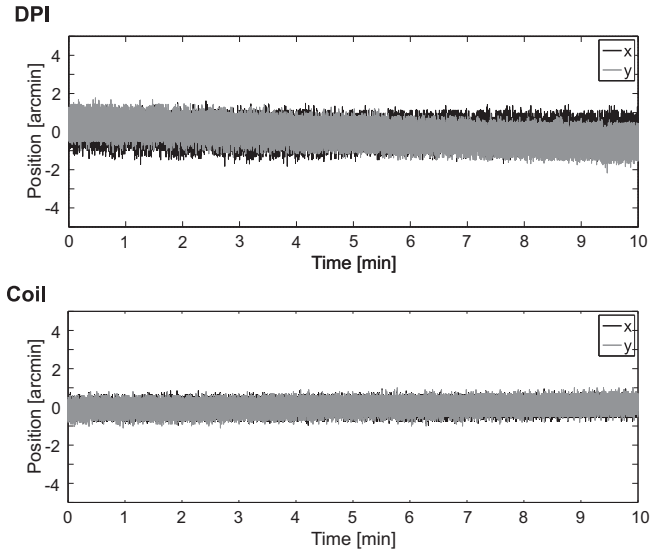

Fig. 3. Slow drift of the eyetrackers. (A) DPI eyetracker. (B) Eye coil. Examples of long-term drifts during recordings of 10 min duration. The total amount of drift was measured as the Euclidean distance between the average position in the first second and the average position in the last second of recording. For the DPI eyetracker, slow drift was 0.07′ per min ±0.029′ ($N = 6$) in amplitude, and it was more pronounced on the vertical (0.062′ per min ±0.032′) than on the horizontal axis (0.027′ per min ±0.012′). For the eye coil, Euclidean distance of drift was 0.069′ per min ±0.034′ ($N = 6$ trials), and vertical drift (0.062′ per min ±0.037′) was greater than horizontal (0.024′ per min ±0.013′).

Table 1
Summary of the noise characteristics (mean ± std).

	RMS instantaneous (arcmin)		Slow drift (arcmin/min)	
	Horizontal	Vertical	Horizontal	Vertical
DPI	0.396 ± 0.094	0.347 ± 0.164	0.027 ± 0.029	0.062 ± 0.032
Eye coil	0.188 ± 0.006	0.194 ± 0.007	0.024 ± 0.013	0.062 ± 0.037

of the model eye with a signal generator that supplied square wave and sine wave inputs to the galvanometer on which the model eye was mounted. As shown in Fig. 4A, a step as small as 1′ (peak to peak amplitude) can be reliably detected by the DPI. Similarly, for a smooth motion like the motion of ocular drift, the system is capable of reliably detecting oscillations at 1 Hz frequency below 2′ in amplitude (see Fig. 4B). These data are consistent with the design specifications (Crane & Steele, 1985), according to which the resolution of the DPI system is 1 arcmin. To determine whether the DPI has, indeed, the capability to reliably resolve gaze shifts in the frequency range of ocular tremor, a square wave signal at 80 Hz with amplitude of 0.5 arcmin was generated. Fig. 4C illustrates an example of recording using this signal. Although we have demonstrated the high resolution of the instrument for purposes of characterizing of ocular drift, we note that it is also crucial for reliable detection of microsaccades.

Coil system. Comparable analyses of system noise and slow drift were performed with the coil system. The eyetracker output was sampled at 1 kHz with a stationary test coil as illustrated in Fig. 1B and the results are shown in Fig. 2B. The noise measured for the coil system was consistently smaller than the noise of the DPI eyetracker (See Table 1). Of most significance were the slow drifts, which had a Euclidean distance of 0.069′ per min. For long experiments, demanding high accuracy in determining retinal position, uncorrected drift could produce significant errors (e.g. 8.4′ in 2 h). Such experiments would benefit from frequent redetermination of a reference position. The noise and drift of

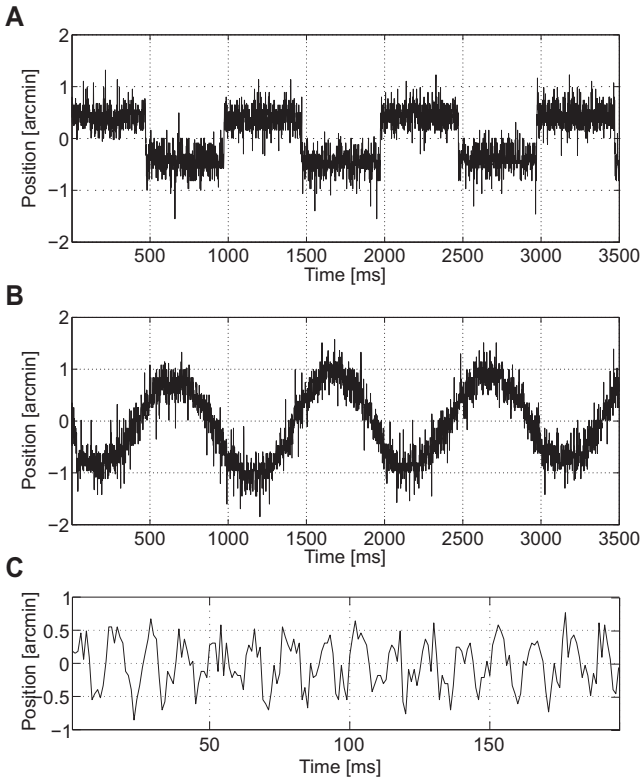

Fig. 4. DPI eyetracker resolution. Eyetracker's output obtained while driving the model eye with different signals: (A) a square wave signal of 1′ (peak-to-peak) amplitude and 1 Hz frequency, (B) a sine wave signal of 2′ amplitude and 1 Hz frequency, (C) a 0.5′ square wave at 80 Hz (C).

the coil system described here are primarily determined by the design and implementation of the electronics.

Measurements of the dynamic response with the test coil were not conducted. However, the mechanical properties of the coil are relatively simple, and measurements of the response of the system with a known voltage input instead of the coil are consistent with the pass-band of 0–320 Hz specified by the manufacturer.

3.2. Temporal frequency characterization of intersaccadic eye movements

DPI system. To determine the impact of system noise on the measures of intersaccadic eye motion we examined the eye movements of 4 human observers during sustained fixation on a blank screen. The power spectrum of human eye movements was compared with the spectrum of the signal recorded with the static model eye. Human eye movement records were segmented into intersaccadic periods (see Methods for details). To achieve high temporal frequency resolution in the computation of the spectrum, only drift periods with duration longer than 3 s were selected ($N = 500$).

Although the power of the eye movements decreased with the temporal frequency, it remained at least two times larger than the power of noise up to 30 Hz (Fig. 5A). The power of the signal then decreased steeply after 80 Hz, and, above 86 Hz, noise and signal were almost indistinguishable (two-tail t-test, $p > 0.05$). These results show that the DPI eyetracker can reliably characterize intersaccadic ocular motion up to ≈80 Hz; the power of the signal was statistically above the level of noise up to 86 Hz (two-tail t-test, $p < 0.001$).

Eye coil system. The power spectrum of intersaccadic epochs of a monkey was compared with the noise of the eye coil system in Fig. 5B. The patterns are very similar to the DPI data from human

subjects including greater power of high frequency tremor on the horizontal axis than the vertical axis. There was slightly greater separation between signal and noise for the coil than for the DPI eyetracker up to ≈40 Hz. Between 50 and 100 Hz the power of the noise in the DPI and in the coil is comparable.

For both systems, and both species, the power of the recorded eye movements is more than twice the noise power over most of the frequency range generally assigned to ocular drift and tremor. Notably, these are the first recordings demonstrating ocular tremor in a non-human primate, and they illustrate the value of refining the eyetracking system to a level that matches the scale of the behavior.

Because the power spectra in Fig. 5 have different resolutions (spectra in Fig. 5A have higher resolution than those in Fig. 5B, see methods for details), to allow for a direct comparison of the temporal characterization of human and non-human intersaccadic motion, we selected intersaccadic periods of comparable duration for the humans and the monkey, and we calculated the power spectrum using the same resolution. Fig. 6 shows that the temporal characteristics of intersaccadic eye movements up to 50 Hz are remarkably similar in the monkey and in humans.

3.3. Characteristics of ocular tremor

Typically, intersaccadic fixational motion is separated into two components: a slow ocular drift component and a higher frequency tremor component of much smaller amplitude (Collewijn & Kowler, 2008; Rolfs, 2010). Although there is no discrete separation between these two components, ocular drift is usually characterized by temporal frequencies up to ≈40 Hz, while tremor occupies a range of temporal frequencies from ≈40 Hz to at least 100 Hz (Adler & Fliegelman, 1934; Bengi & Thomas, 1968; Bolger et al., 1999; Coakley, 1983; Ditchburn & Ginsborg, 1953; Eizenman et al., 1985; Ratliff & Riggs, 1950; Riggs, Armington, & Ratliff, 1954; Matin, 1964; Spauschus et al., 1999). Within this range, the dominant frequency of tremor is known to vary across subjects (Bolger et al., 1999).

Estimates of the amplitude of tremor, although small in magnitude, still vary widely. Eizenman et al. (1985) reported the peak amplitude of tremor to be only 6 arcsec, whereas Ratliff and Riggs (1950) found a median amplitude of 17.5 arcsec and individual samples at least as large as 1′. Here we show that eye movements in the frequency range of ocular tremor can be reliably characterized both with the DPI and the coil system.

DPI system: human data. The tremor component is visible in the eye movements power spectrum in the range between 40 and 80 Hz. As illustrated in Fig. 5A, tremor was more pronounced on the horizontal axis than on the vertical axis of motion. Moreover, as shown in Fig. 7A, there are differences among human subjects in the amount of tremor. However, for each observer, the frequency range associated with the highest power, remained

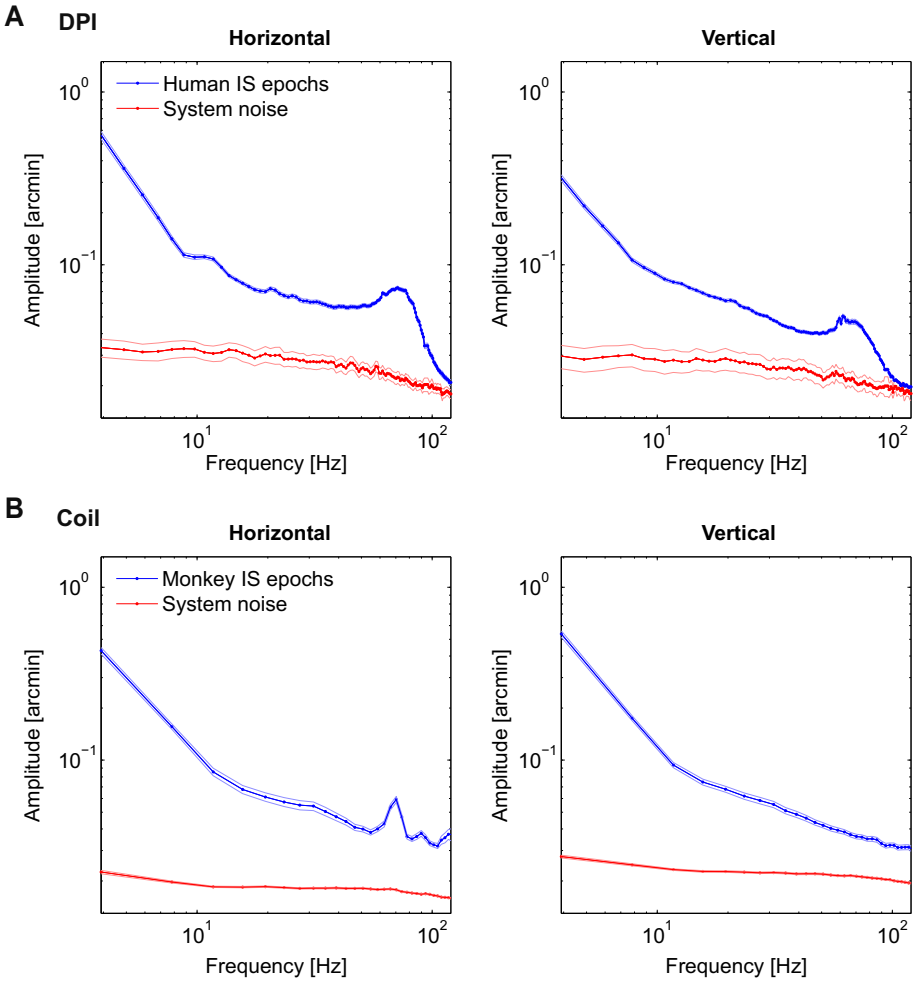

Fig. 5. Power spectrum of intersaccadic eye motion. (A) Spectral density for the horizontal and vertical components of human ocular drift and tremor (blue) measured with a DPI. For comparison, the spectrum of the system noise (red) recorded with a static model eye is also shown. Estimates were obtained from 36 epochs of 10 s duration for the model eye and 500 drift segments (>3 s) recorded during sustained fixation from four human observers. (B) Power spectra measured for the monkey using the eye coil ($N = 490$ drift segments >384 ms). Data are compared to the spectral density of noise recorded with a stationary test coil (360 recordings of 5 s duration). Error bars represent 95% confidence intervals. (For interpretation of the references to color in this figure legend, the reader is referred to the web version of this article.)

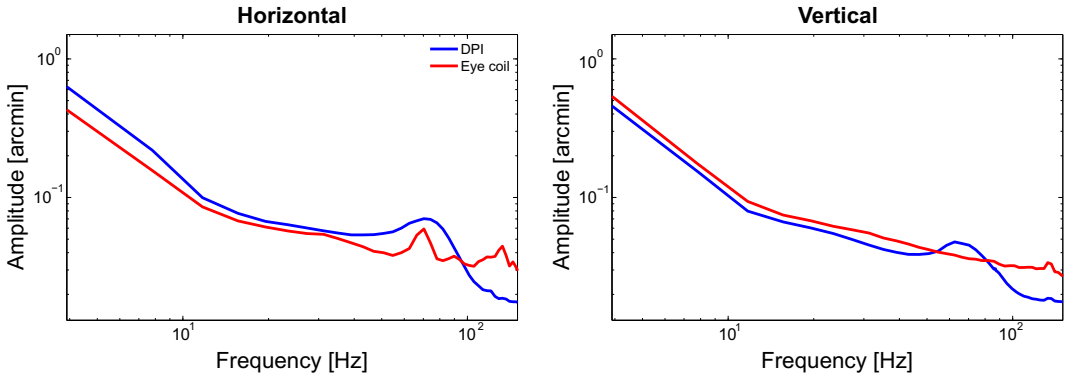

Fig. 6. Comparison of spectral estimates. Power spectra of the intersaccadic eye movements were estimated using fixation segments of similar duration in both the monkey ($N = 490$ drift segments) and humans ($N = 6927$ drift segments). See Methods for details.

approximately the same across different drift segments and different recording sessions.

We examined the tremor by filtering the eye movement signal using a band-pass filter with a frequency range of 40 and 80 Hz. As illustrated in Fig. 7C, the standard deviation of the filtered eye movement signal was much higher than the standard deviation of the filtered noise (0.22′ vs. 0.07′ on the horizontal axis, and 0.15′ vs. 0.07′ on the vertical axis). These findings, once again, show that ocular tremor can be characterized using a DPI eyetracker as its amplitude is higher than the amplitude of the noise in that frequency range.

Interestingly, the horizontal component of tremor is greater than the vertical component for both the humans and the monkey. There is little information from previous studies about possible differences on the horizontal and vertical axes. Both Eizenman et al. (1985) and Spauschus et al. (1999) measured only horizontal eye movements, and Stevenson et al. (2010) only show the spectrum for horizontal eye movements. These differences cannot be explained by off-axes fixation as the fixated location on the display was always perpendicular to the line of sight. However, for the DPI recordings, the amplitude of eye motion in between 0 and 50 Hz was also smaller on the vertical compared to the horizontal axis, it is, therefore, not surprising that the magnitude of tremor followed the same pattern. Vertical and horizontal eye motion are controlled by different sets of extraocular muscles; if tremor is a byproduct of the firing of motor neurons, as originally hypothesized by Eizenman et al. (1985), it is then possible that different firing intensities, probably associated with larger horizontal fixational displacements, lead to differences in the horizontal and vertical magnitude of tremor. Another possibility is that, as proposed by Riggs and Ratliff (1951), involuntary tremor naturally occurs when balancing the eyeball between pairs of antagonistic muscles. Differences in muscles imbalances in different pairs of muscles might then lead to different tremor intensities.

Coil system: monkey data. For the monkey, like humans, tremor was greater on the horizontal axis. For averaged data collected on two days one week apart (Fig. 5B), there was a noticeable peak localized around ≈68 Hz, and, differently from humans, the frequency associated with this peak varied in unpredictable ways from one session to another (Fig. 7B). The dominant frequency usually was fairly similar over short time periods (Day 1, sessions 2 and 3), but it could be quite different on a subsequent day (Day 2), and systematically shift within a day (Day 2, sessions 1 and 2) or dramatically shift after a 30 min pause on the same day (Day 2 session 2 to Day 2 session 3). These changes in the spectral content are clear enough to be noticeable even in the raw records, as illustrated in the example traces in the right column.

It has been proposed that ocular tremor is a byproduct of the regularity of firing patterns of the oculomotor neurons and is a function of eye position (Eizenman et al., 1985). However, the dominant frequency of tremor varied over a wide range while the monkey's scatter of eye position had a standard deviation of only 2.6 arcmin horizontally and 3.2 arcmin vertically. Thus, the variations in eye position were so small that they cannot plausibly explain the variations in frequency of tremor.

3.4. Estimation of intersaccadic ocular speed

The results shown so far were based on the raw data acquired with the coil and the DPI system. In principle, the impact of noise on the eyetracker output can be reduced by judicious filtering of the signal. The signal-to-noise ratio and the frequency components during the intersaccadic epochs should provide a rationale for determining the optimal cut-off frequency when filtering the signal.

DPI system. Based on the results obtained with the DPI system, a low pass filter with a conservative cut-off at ≈80 Hz would remove the components of the recordings where the signal overlaps with noise, while preserving the slow drift component of the eye movement signal, as well as most of the ocular tremor. Note that these cut-offs may not apply to all instruments because they depend on the noise characteristics of the individual eyetracking device. Given the temperamental nature of analog systems, it is important to monitor the DPI noise regularly with a model eye to ensure that the chosen cut-off frequency remains appropriate. On the other hand, if only the slow drift component is of interest, a more conservative cut-off frequency of ≈30–40 Hz can be applied.

Here, to filter eye movements during intersaccadic periods, we used a third-order Savitzky-Golay filter; this method performs a local polynomial regression and was preferred over more traditional filters because of its higher stability during the initial and final intervals of each drift segment (Savitzky & Golay, 1964). Fig. 8A shows an example of a raw eye movement trace during an intersaccadic period and of the same trace filtered with a low-pass Savitzky-Golay with a frequency cut-off of ≈80 Hz.

Coil system. The same considerations apply when evaluating the application of a filter to data collected with the coil system. In Fig. 8B we provide parallel illustrations of intersaccadic movements of the monkey processed in the same way as the human data. In general, the results are similar to the human data, but as a result of the higher power characterizing the monkey's intersaccadic motion in the tremor range, a cutoff of 100 Hz could be used when filtering the eye movements.

Filtering the raw data acquired with the eyetracking system has the immediate impact of changing the estimation of the speed of eye movements during the intersaccadic epochs. As shown in

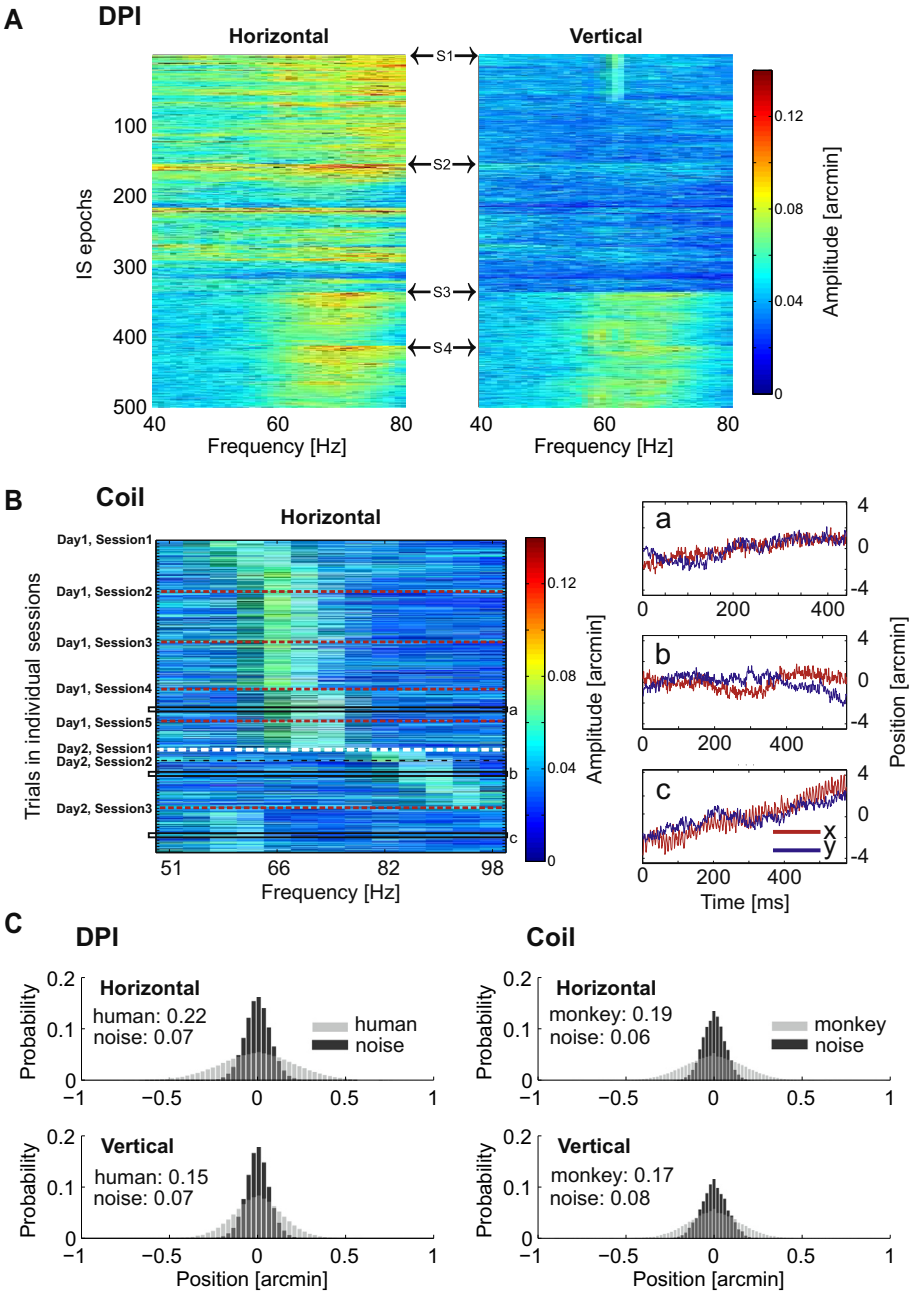

Fig. 7. Frequency variation of ocular tremor. (A) DPI eyetracker. Distribution of spectral power from 40 to 100 Hz (tremor) in intersaccadic epochs for 4 human subjects (S1–4). Each row represents the spectrum of one intersaccadic segment for the horizontal (left) and the vertical (right) components of ocular motion. The order of the segments within the session is preserved, but only segments sufficiently long (>3 s) for spectral estimation are shown. (B) Eye coil. Raster of spectral power of the horizontal component of ocular motion in a succession of intersaccadic epochs ($N = 490$, duration >384 ms) recorded for the monkey during fixation trials of 3 s duration. Data from 8 recording sessions conducted over 2 days. Red dashed lines indicate start of a new session. For most sessions about 5 min elapsed before beginning the next session. For two sessions (Day 1, Session 4; Day 2 Session 3) ≈30 min elapsed between sessions. The dashed white line indicates passage of a full day before the new session. Thin black rectangles designate selected intersaccadic epochs plotted to the right, showing eye position vs. time for individual epochs with high power centered around (a) ≈70 Hz, (b) ≈90 Hz, (c) ≈60 Hz. Horizontal eye position is plotted in red, vertical in blue. (C) Histograms of eye position during the intersaccadic interval (light gray bars) compared with histograms of system noise (dark gray bars). The mean eye position was subtracted from each intersaccadic epoch and from the noise recordings and both eye movements and the noise have been filtered with a band-pass of 40–80 Hz to emphasize ocular tremor. Numbers in the graphs represent standard deviations. (For interpretation of the references to color in this figure legend, the reader is referred to the web version of this article.)

Fig. 9, lower cut-off frequencies yield lower speed estimates. Even when using a conservative cut-off frequency of 30 Hz, the intersaccadic speed is ≈33 arcmin/s, which is significantly higher than previous estimates (Bennet-Clark, 1964; Boyce, 1967; Ditchburn, 1973; Fiorentini & Ercoles, 1966; Krauskopf et al., 1960; Nachmias, 1959; Rattle, 1969; Sansbury et al., 1973; Skavenski, Hansen, Steinman, & Winterson, 1979; Skavenski & Steinman, 1970; Steinman, 1965). When using a cut-off frequency of 80 Hz, the estimate of median intersaccadic speed is even higher –about 1.5 deg/s– and upper limit can be as high as 4 deg/s. Importantly, these findings are robust, being very similar when recorded with different methods, and even in different species (compare Fig. 9A and B). Therefore, with appropriate filtering, the contributions of ocular drift and tremor to retinal motion become apparent.

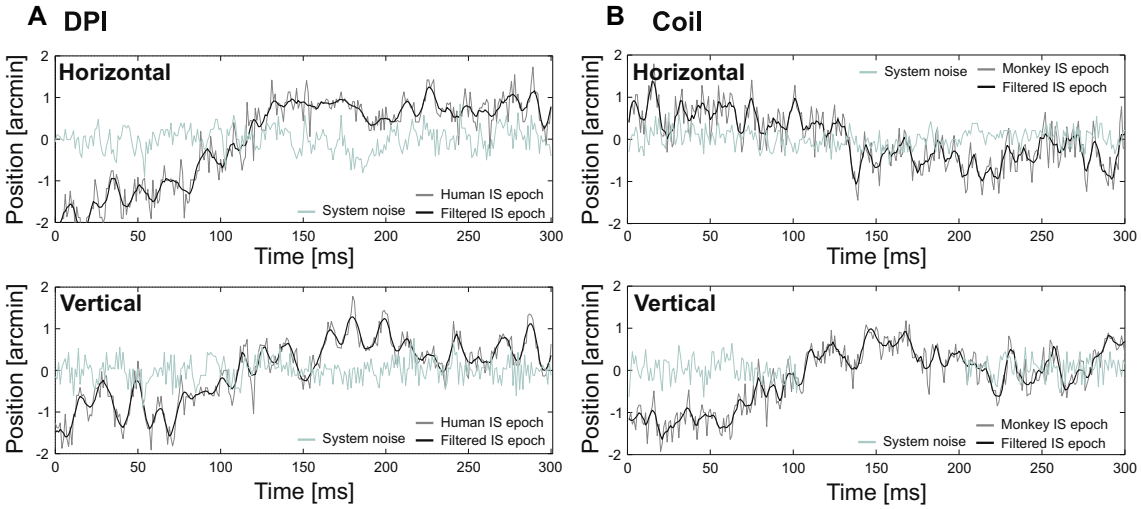

Fig. 8. Examples of intersaccadic eye movements. (A) DPI recording from a human observer. (B) Eye coil recording from a monkey. In both cases, the two panels show horizontal (top) and vertical (bottom) movements. Gray traces represent the raw data while black traces represent the same data filtered with a low-pass Savitzky-Golay filter over 15 samples (≈80 Hz cut-off). Light blue traces indicate the noise signal recorded with the static model eye or eye coil. Note that individual filtered traces may deviate from the overall spectral characteristics of tremor. (For interpretation of the references to color in this figure legend, the reader is referred to the web version of this article.)

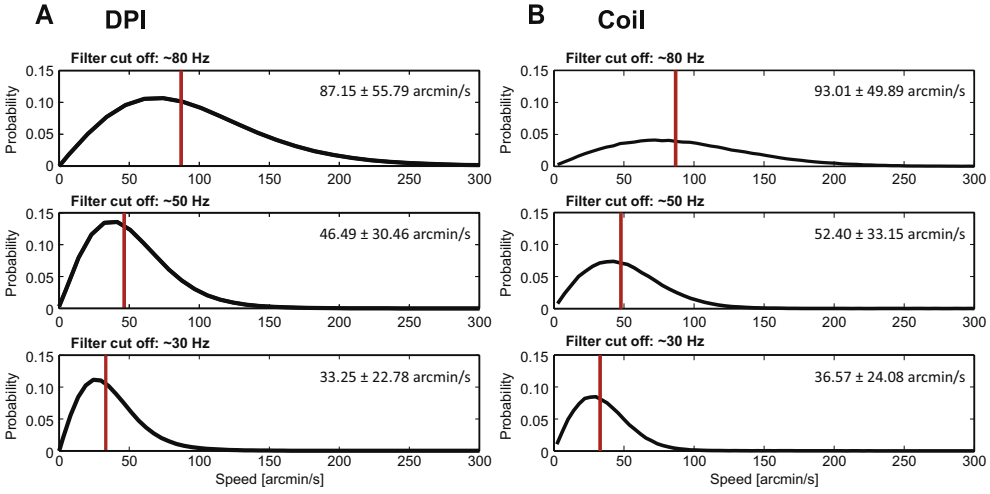

Fig. 9. Ocular speed during intersaccadic epochs. Ocular speed distributions for the same set of intersaccadic data as in Figs. 5 and 7. (A) Human data acquired with a DPI eyetracker. (B) Monkey data acquired with an eye coil. Each row shows data filtered with Savitzky-Golay low pass filters with different cut-off frequencies. The vertical red lines and the insets in the graphs indicate the medians of the distribution. (For interpretation of the references to color in this figure legend, the reader is referred to the web version of this article.)

4. Discussion

We examined the performance of DPI and scleral coil eyetracking methods in measuring intersaccadic eye movements. We used a test coil and a model eye to assess the level of noise in the two systems, and compared noise characteristics to the intersaccadic eye motion measured with human subjects for the DPI, and with a non-human primate for the coil. We show that the spectral power of the recorded eye movements is much larger than that of noise over a very broad frequency range that extends up to 80 Hz. Our results suggest that both these systems possess sufficiently high precision and resolution to record ocular drift and tremor during fixation.

DPI eyetracker. Our analysis confirms that the DPI is a very powerful system for measuring small eye movements. Several words of caution are, however, necessary. The artificial eye measurements described here should be taken as a limit of the system under ideal conditions. While the use of a model eye in the assessment of performance is essential, it is important to keep in mind that other factors may further lower precision when recording real eye movements. Clearly, a model eye does not capture a number of potential artifacts associated with a biological eye, and very little is known about the possible influences on DPI recordings of factors such as lens accommodation, changes in pupil size, perisaccadic lens wobble (Deubel & Bridgeman, 1995a, 1995b; Stevenson & Roorda, 2005; Tabernero & Artal, 2014), eye torsion, the presence of a tear film and small head movements.

Our experiments were conducted under conditions specifically designed to minimize the possible influence of the previous factors. Perisaccadic lens wobble artifacts were eliminated by discarding perisaccadic events and by examining only periods of steady fixation. We also limited accommodation factors by maintaining the fixated region always at the same location and distance from the subject throughout the recording time. While we cannot completely eliminate the influence of accommodative fluctuations, torsional motion and the presence of a tear film, possible artifacts

generating from these factors are likely to affect the spectrum in the low temporal frequency range (*e.g.*, 1–2 Hz for lens accommodation (Campbell, Robson, & Westheimer, 1959; Kotulak & Schor, 1986)). This is the frequency band in which the power of the signal is higher and therefore also likely to be less susceptible to such artifacts.

The DPI eyetracker is relatively robust to small head translation and changes in pupil size within a limited range (Crane & Steele, 1985). Yet, to further limit possible artifacts due to minute head movements, the subject's head was immobilized by means of a head-rest and a bite-bar during data collection. A bite-bar guarantees much more head stability than the widely-used chin-rest, and its use is highly recommended when studying intersaccadic eye movements, unless a system specifically designed to handle head movements is used (*e.g.* Epelboim et al. (1995)). Pupil changes could also influence DPI recordings, as the fourth Purkinje image is no longer visible when the pupil constricts to small diameters. To circumvent this issue, we always ensured its full visibility in our measurements. Eye movements were collected in a relatively dimly illuminated room, and the display was maintained at the same level of contrast and luminance throughout the recording period. In keeping with these observations, the similarity between the spectra estimated from eye-coil and DPI data supports the notion that these factors minimally affect DPI measurements.

Eye coil. Although the eye coil is by design immune to most of the factors mentioned above, there are a number of elements that should be controlled to optimize its performance. To this end, we paid closed attention to several aspects of the eye coil system. The strength of the magnetic field at the center of the field coil was maximized by using the maximum current of the power amplifiers with enlarged heat sinks. While for human use, a field coil that is 60 cm on a side is a typical configuration and it is often used for animals, in our system, the field coil size was reduced to a cube 50 cm on a side, which produces higher field strength. A possible source of noise in the eye coil is pickup in the cables connecting the eye coil to the main amplifier. In the EM7 system the effect of this noise source is minimized by placing a preamplifier (Fig. 1) close to the eye coil and by supporting the cables so that they do not touch the field coil and they could not move during the recording. Low frequency artifacts can be produced by movement of the leads of the eye coil by muscles and skin outside the eye, but along the path of the lead to the connector. To reduce these artifacts we placed the leads to minimize effects of muscular movements such as chewing or licking. And recordings were not made in inter-trial intervals while the monkey was consuming its liquid reward. Artifacts could also result from strong air currents passing over the eye coil leads as they emerge from the implant. We conducted control experiments with the test coil by blocking air currents to confirm that such artifacts did not affect our measurements.

It is worth observing that, the way eye movements recordings are acquired in human and non-human primates by means of the eye coil differs. In our experiments, we used a search coil 14 mm in diameter with 3 turns of wire, sutured to the sclera of the monkey's eye. For human experiments, search coils are embedded in a silicone rubber ring that adheres to the sclera by capillary and suction forces (Chronos Vision, Berlin, Germany). The human search coil is 18 mm in diameter and it has 9 turns of wire. The voltage induced in the coil is proportional to the enclosed area and the number of turns. Thus, with the same field strength, the human coil should produce substantially greater voltage and hence even better signal-to-noise ratios than the monkey coil that we have used.

Reports from the literature are consistent with high accuracy and precision in human experiments with the coil system. Noise levels are reported to be less than 1 arcmin peak-to-peak with a bandwidth of 200 Hz (Deubel & Bridgeman, 1995a) and about 0.5 arcmin with a bandwidth of 100 Hz (Collewijn, van der Mark, & Jansen, 1975). Perhaps the largest potential error is the risk that the ring containing the coil slips on the eye, but the suction holding the ring on the eye is reported to be so strong that the ring must be removed by blunt forceps (Collewijn et al., 1975). We are not aware of reports or analyses of errors being caused by slippage of the ring.

Although human eye coils are capable of high standards of performance, their use is limited because they are invasive. The cornea must be anesthetized, and even then the ring cannot be tolerated for more than about 30–60 min. These are some of the reasons why so many experiments are now performed with video eyetrackers, which are noninvasive and easy to use. One of our goals is to provide measures of performance that are useful for evaluating any eyetracking system and determining the applications for which it is appropriate.

Although the eye coil and the DPI represent two of the most reliable and precise techniques to record eye movements during intersaccadic periods, other techniques can now achieve comparable standards and hold great promise. In particular image-based eyetracking based on AOSLO technology has proven to be as good as the DPI and less susceptible to lens-wobble artifacts (Stevenson et al., 2010, Stevenson, Sheehy, & Roorda, 2015).

Estimation of intersaccadic speed. Since differentiation is a delicate operator that amplifies the noise, particular care needs to be dedicated to the estimation of velocity. Filtering is necessary before attempting numerical differentiation of the position signals. In this study, we carefully selected our filter on the basis of the noise estimates. We first determined the maximum frequency at which the signal could be reliably discriminated from the noise, and then filtered accordingly. Our general remarks are that, an optimal filter should be based on (*a*) a characterization of the noise level; (*b*) the component of intersaccadic motion one is interested in examining. To selectively study ocular drift component a cut-off between 30 and 40 Hz maybe sufficient, provided that the noise level is below the power of the eye movement signal within this range. Choice of higher cut-off frequencies must be based on a careful examination of the signal-to-noise ratio given by the eyetracker.

The experimenter should also keep in mind that the choice of the filter, which needs to be made explicit in publications, will have an impact on estimates of the speed of intersaccadic motion. Consistent with previous findings (Cherici et al., 2012), we measured a drift speed close to 1 deg/s when data were low-pass filtered with a cut-off frequency of ≈50 Hz. The same data yield an average speed of almost 2 deg/s when the cut-off frequency is raised to ≈80 Hz. Strikingly similar estimated were obtained with eye coil data from the macaque. Therefore, the speed of retinal motion during fixation is much higher than normally thought.

Ocular tremor. Even if based on different recording techniques, our results are in strong agreement with those of Eizenman et al. (1985) and Spauschus et al. (1999). They show a clear deviation in the intersaccadic spectrum from the $1/F^2$ (F represents temporal frequency) trend above 40 Hz. Moreover, they show a close correspondence between oculomotor characteristics of humans and a rhesus monkey in the range 0–50 Hz, indicating that differences in the recording techniques did not have a major impact on the characteristics of intersaccadic motion. Some differences were visible above 50 Hz, in the range of tremor, which was more pronounced in humans than in the tested monkey, particularly on the vertical axis of motion. Whether this represents an individual difference, a species difference, or possible attenuation of tremor caused by the presence of the coil in the eye, will need to be address by future studies.

While a number of studies have examined the characteristics of ocular drift (Cherici et al., 2012; Ditchburn, 1973; Engbert & Kliegl, 2004; Fiorentini & Ercoles, 1966; Krauskopf et al., 1960; Kuang

et al., 2012; Nachmias, 1959; Nachmias, 1961; Rattle, 1969; Rucci et al., 2007; Steinman, 1965; Skavenski & Steinman, 1970; Steinman et al., 1973; Sansbury et al., 1973), ocular tremor has not been investigated to the same extent. In fact, ocular tremor is often ignored by oculomotor studies. This happens primarily because the eyetracking system is not sufficiently accurate to measure it, or because it is a priori discarded as noise. Although small, tremor shifts synchronously the image over the entire retina, a motion that could lead to neural responses (*e.g.* Greschner, Bongard, Rujan, & Ammermuller (2002), Maldonado et al. (2008)). As noted by Ahissar and Arieli (2001), the temporal frequency of ocular tremor falls within the gamma-band of oscillations that contribute to neuronal synchrony in many areas of the brain (Buzsaki, 2006). It would be very interesting to know how ocular tremor might trigger or otherwise interact with the gamma oscillations in the visual system. These considerations point to the need for a better understanding of ocular tremor, the differences between individuals, and possible variations within the same individual over time. Our study shows that, with great care, both the DPI and coil systems can be pushed to their limits and can be used to further investigate ocular tremor.

Acknowledgements

The authors thank M. Rucci for helpful comments. This work was supported by National Science Foundation grant BCS 1534932 to MP and grant IOS 0843354 to DMS, and by the National Institutes of Health grant EY18363.

References

Adler, F. H., & Fliegelman, M. (1934). Influence of fixation on the visual acuity. *Archives of Ophthalmology, 12*, 475–483.
Ahissar, E., & Arieli, A. (2001). Figuring space by time. *Neuron, 32*, 185–201.
Ahissar, E., & Arieli, A. (2012). Seeing via miniature eye movements: A dynamic hypothesis for vision. *Frontiers in Computational Neuroscience, 6*, 1–27.
Arend, L. E. (1973). Spatial differential and integral operations in human vision: Implications of stabilized retinal image fading. *Psychological Review, 80*, 374–395.
Averill, H. I., & Weymouth, F. W. (1925). Visual perception and the retinal mosaic, II. The influence of eye movements on the displacement threshold. *Journal of Comparative Psychology, 5*, 147–176.
Awal, M., Mostafa, S., & Ahmad, M. (2011). Performance analysis of Savitzky–Golay smoothing filter using ECG signal. *International Journal of Computer and Information Technology, 1*, 24–29.
Aytekin, M., Victor, J. D., & Rucci, M. (2014). The visual input to the retina during natural head-free fixation. *Journal of Neuroscience, 34*, 12701–12715.
Bedell, H. E., & Stevenson, S. B. (2013). Eye movement testing in clinical examination. *Vision Research, 90*, 32–37.
Bengi, H., & Thomas, J. G. (1968). Fixation tremor in relation to eyeball-muscle mechanics. *Nature, 217*, 773–774.
Bennet-Clark, H. C. (1964). The oculomotor response to small target replacements. *Optica Acta, 11*, 301–314.
Bolger, C., Bojanic, S., Sheahan, N. F., Coakley, D., & Malone, J. F. (1999). Dominant frequency content of ocular microtremor from normal subjects. *Vision Research, 39*, 1911–1915.
Boyce, P. R. (1967). Monocular fixation in human eye movement. *Proceedings of the Royal Society of London. Series B, Biological Sciences, 167*, 293–315.
Burak, Y., Rokni, U., Meister, M., & Sompolinsky, H. (2010). Bayesian model of dynamic image stabilization in the visual system. *Proceedings of the National Academy of Sciences, USA, 107*, 19525–19530.
Buzsaki, G. (2006). *Rhythms of the brain*.Oxford: Oxford University Press.
Campbell, F., Robson, J., & Westheimer, G. (1959). Fluctuations of accommodation under steady viewing conditions. *The Journal of Physiology, 145*, 579–594.
Cherici, C., Kuang, X., Poletti, M., & Rucci, M. (2012). Precision of sustained fixation in trained and untrained observers. *Journal of Vision, 12*, 1–16.
Choe, K. W., Blake, R., & Lee, S. H. (2016). Pupil size dynamics during fixation impact the accuracy and precision of video-based gaze estimation. *Vision Research, 118*, 48–59.
Coakley, D. (1983). *Minute eye movement and brain stem function*. CRC Press.
Collewijn, H., & Kowler, E. (2008). The significance of microsaccades for vision and oculomotor control. *Journal of Vision, 8*, 1–21.
Collewijn, H., van der Mark, F., & Jansen, T. C. (1975). Precise recording of human eye movements. *Vision Research, 15*, 447–450.
Crane, H. D., & Steele, C. (1978). Accurate three-dimensional eyetracker. *Applied Optics, 17*, 691–705.
Crane, H. D., & Steele, C. (1985). Generation V dual Purkinje-image eyetracker. *Applied Optics, 24*, 527–537.
Desbordes, G., & Rucci, M. (2007). A model of the dynamics of retinal activity during natural visual fixation. *Visual Neuroscience, 24*, 217–230.
Deubel, H., & Bridgeman, B. (1995a). Fourth Purkinje image signals reveal eye-lens deviations and retinal image distortions during saccades. *Vision Research, 35*, 529–538.
Deubel, H., & Bridgeman, B. (1995b). Perceptual consequences of ocular lens overshoot during saccadic eye movements. *Vision Research, 35*, 2897–2902.
Ditchburn, R. W. (1973). *Eye movements and visual perception*.Oxford: Clarendon Press.
Ditchburn, R. W., & Ginsborg, B. L. (1953). Involuntary eye movements during fixation. *The Journal of Physiology, 119*, 1–17.
Drewes, J., Masson, G. S., & Montagnini, A. (2012). Shifts in reported gaze position due to changes in pupil size: Ground truth and compensation. In *Proceedings of the symposium on eye tracking research and applications* (pp. 209–212). New York, NY, USA: ETRA.
Drewes, J., Zhu, W., Hu, Y., & Hu, X. (2014). Smaller is better: Drift in gaze measurements due to pupil dynamics. *PLoS ONE, 9*, e111197.
Eizenman, M., Hallett, P., & Frecker, R. (1985). Power spectra for ocular drift and tremor. *Vision Research, 25*, 1635–1640.
Engbert, R., & Kliegl, R. (2004). Microsaccades keep the eyes' balance during fixation. *Psychological Science, 15*, 431–436.
Engbert, R., Mergenthaler, K., Sinn, P., & Pikovsky, A. (2011). An integrated model of fixational eye movements and microsaccades. *Proceedings of the National Academy of Sciences, USA, 108*, 765–770.
Epelboim, J., Kowler, E., Steinman, R. M., Collewijn, H., Erkelens, C. J., & Pizlo, Z. (1995). When push comes to shove: Compensation for passive perturbation of the head during natural gaze shifts. *Journal of Vestibular Research, 5*, 421–442.
Fiorentini, A., & Ercoles, A. M. (1966). Involuntary eye movements during attempted monocular fixation. In *Atti Fondazione Giorgio Ronchi* (pp. 199–217).
Gorry, P. (1990). General least-squares smoothing and differentiation by the convolution (Savitzky-Golay) method. *Analytical Chemistry, 62*, 570–573.
Greschner, M., Bongard, M., Rujan, P., & Ammermuller, J. (2002). Retinal ganglion cell synchronization by fixational eye movements improves feature estimation. *Nature, 5*, 341–347.
Haslinger, R., Pipa, G., Lima, B., Singer, W., Brown, E. N., & Neuenschwander, S. (2012). Context matters: The illusive simplicity of macaque V1 receptive fields. *PLoS ONE, 7*, e39699.
Holmqvist, K., Nystrom, M., Andersson, R., Dewhurst, R., Jarodzka, H., & de Weijer, J. V. (2011). *Eye tracking: A comprehensive guide to methods and measures*. Oxford University Press.
Houben, M. M., Goumans, J., & van der Steen, J. (2006). Recording three-dimensional eye movements: scleral search coils versus video oculography. *Investigative Ophthalmology & Visual Science, 47*, 179–187.
Judge, S. J., Richmond, B. J., & Chu, F. C. (1980). Implantation of magnetic search coils for measurement of eye position: An improved method. *Vision Research, 20*, 535–538.
Kagan, I., Gur, M., & Snodderly, D. M. (2008). Saccades and drifts differentially modulate neuronal activity in V1: Effects of retinal image motion, position, and extraretinal influences. *Journal of Vision, 8*, 1–25.
Kimmel, D. L., Mammo, D., & Newsome, W. T. (2012). Tracking the eye non-invasively: Simultaneous comparison of the scleral search coil and optical tracking techniques in the macaque monkey. *Frontiers in Behavioral Neuroscience*, 6.
Kolakowski, S., & Pelz, J. B. (2006). Compensating for eye tracker camera movement. In *Proceedings of the ACM SIGCHI eye tracking research & applications symposium*, San Diego, California, United States. .
Kotulak, J., & Schor, C. (1986). Temporal variations in accommodation during steady-state conditions. *Journal of Optical Society of America, Series A, 3*, 223–227.
Krauskopf, J., Cornsweet, T. N., & Riggs, L. A. (1960). Analysis of eye movements during monocular and binocular fixation. *Journal of the Optical Society of America, 50*, 572–578.
Kuang, X., Poletti, M., Victor, J. D., & Rucci, M. (2012). Temporal encoding of spatial information during active visual fixation. *Current Biology, 20*, 510–514.
Maldonado, P., Babul, C., Singer, W., amd, D., Berger, E. R., & Grun, S. (2008). Synchronization of neuronal responses in primary visual cortex of monkeys viewing natural images. *Journal of Neurophysiology, 100*, 1523–1532.
Marshall, W. H., & Talbot, S. A. (1942). Recent evidence for neural mechanisms in vision leading to a general theory of sensory acuity. In H. Kluver (Ed.), *Biological symposia—Visual mechanisms* (Vol. 7, pp. 117–164). Lancaster, PA: Cattle.
Matin, L. (1964). Measurement of eye movements by contact lens techniques: Analysis of measuring systems and some new methodology for three-dimensional recording. *Journal of the Optical Society of America, 54*, 1008–1018.
Merchant, J., Morrissette, R., & Porterfield, J. L. (1974). Remote measurement of eye direction allowing subject motion over one cubic foot of space. *Transactions on Biomedical Engineering, 21*, 309–317.
Nachmias, J. (1959). Two-dimensional motion of the retinal image during monocular fixation. *Journal of the Optical Society of America, 49*, 901–908.
Nachmias, J. (1961). Determiners of the drift of the eye during monocular fixation. *Journal of the Optical Society of America, 51*, 761–766.
Nystrom, M., Andersson, R., Holmqvist, K., & van de Weijer, J. (2013). The influence of calibration method and eye physiology on eyetracking data quality. *Behavior Research Methods, 45*, 272–288.

Poletti, M., & Rucci, M. (2016). A compact field guide to the study of microsaccades: Challenges and functions. *Vision Research, 118*, 83–97.
Ratliff, F., & Riggs, L. A. (1950). Involuntary motions of the eye during monocular fixation. *Journal of Experimental Psychology, 40*, 687–701.
Rattle, J. D. (1969). Effect of target size on monocular fixation. *Optica Acta, 16*, 183–190.
Remmel, R. S. (1984). An inexpensive eye movement monitor using the scleral search coil technique. *Transactions on Biomedical Engineering, 31*, 388–390.
Riggs, L. A., Armington, J. C., & Ratliff, F. (1954). Motions of the retinal image during fixation. *Journal of the Optical Society of America, 44*, 315–321.
Riggs, L., & Ratliff, F. (1951). Visual acuity and the normal tremor of the eyes. *Science, 114*, 17–18.
Robinson, D. A. (1963). A method of measuring eye movement using scleral search coil in a magnetic field. *IEEE Transactions on Biomedical Engineering, 10*, 137–145.
Rolfs, M. (2010). Microsaccades: Small steps on a long way. *Vision Research, 49*, 2415–2441.
Rucci, M., & Casile, A. (2004). Decorrelation of neural activity during fixational instability: Possible implications for the refinement of V1 receptive fields. *Visual Neuroscience, 21*, 725–738.
Rucci, M., Iovin, R., Poletti, M., & Santini, F. (2007). Miniature eye movements enhance fine spatial detail. *Nature, 447*, 852–855.
Rucci, M., & Poletti, M. (2015). Control and function of fixational eye movements. *Annual Review of Vision Science, 1*, 499–518.
Rucci, M., & Victor, J. D. (2015). The unsteady eye: An information processing stage, not a bug. *Trends in Neurosciences, 38*, 195–206.
Sansbury, R. V., Skavenski, A. A., Haddad, G. M., & Steinman, R. M. (1973). Normal fixation of eccentric targets. *Journal of the Optical Society of America, 63*, 612614.
Santini, F., Redner, G., Iovin, R., & Rucci, M. (2007). EyeRIS: A general-purpose system for eye movement contingent display control. *Behavioral Research Methods, 39*, 350–364.
Savitzky, A., & Golay, M. J. E. (1964). Smoothing and differentiation of data by simplified least squares procedures. *Analytic Chemistry, 36*, 1627–1639.
Sheehy, C., Yang, Q., Arathorn, D., Tiruveedhula, P., de Boer, J., & Roorda, A. (2012). High-speed, image-based eye tracking with a scanning laser ophthalmoscope. *Biomedical Optics Express, 3*, 2611–2622.
Skavenski, A. A., Hansen, R. M., Steinman, R. M., & Winterson, B. J. (1979). Quality of retinal image stabilization during small natural and artificial body rotations in man. *Vision Research, 19*, 675–683.
Skavenski, A. A., & Steinman, R. M. (1970). Control of the eye position in the dark. *Vision Research, 10*, 193–203.
Snodderly, D. M. (2016). A physiological perspective on fixational eye movements. *Vision Research, 118*, 31–47.
Snodderly, D. M., Kagan, I., & Gur, M. (2001). Selective activation of visual cortex neurons by fixational eye movements: Implications for neural coding. *Visual Neuroscience, 18*, 259–277.
Spauschus, A., Marsden, J., Halliday, D. M., Rosenberg, J. R., & Brown, P. (1999). The origin of ocular microtremor in man. *Experimental Brain Research, 126*, 556–562.
Steinman, R. M. (1965). Effect of target size, luminance, and color on monocular fixation. *Journal of the Optical Society of America, 55*, 1158–1165.
Steinman, R. M., & Collewijn, H. (1980). Binocular retinal image motion during active head rotation. *Vision Research, 20*, 415–429.
Steinman, R. M., Haddad, G. M., Skavenski, A. A., & Wyman, D. (1973). Miniature eye movement. *Science, 181*, 810–819.
Stevenson, S., & Roorda, A. (2005). Correcting for miniature eye movements in high resolution scanning laser ophthalmoscopy. In F. Manns, P. Soderberg, & A. Ho (Eds.), *Ophthalmic technologies XV* (pp. 145–151). SPIE.
Stevenson, S. B., Roorda, A., & Kumar, G. (2010). Eye tracking with the adaptive optics scanning laser ophthalmoscope. In S. N. Spencer (Ed.), *Proceedings of the 2010 symposium on eye-tracking research and applications* (pp. 195–198). New York: Association for Computed Machinery.
Stevenson, S., Sheehy, C., & Roorda, A. (2015). Binocular eye tracking with the tracking scanning laser ophthalmoscope. *Vision Research, 118*, 98–104.
Tabernero, J., & Artal, P. (2014). Lens oscillations in the human eye. Implications for post-saccadic suppression of vision. *PLoS ONE, 9*, e95764.
Vinje, W. E., & Gallant, J. L. (2000). Sparse coding and decorrelation in primary visual cortex during natural vision. *Science, 287*, 1273–1276.
Welch, P. (1967). The use of fast fourier transform for the estimation of power spectra: A method based on time averaging over short, modified periodograms. *IEEE Transactions on Audio Electroacoustics, AU-15*, 70–73.
Wildenmann, U., & Schaeffel, F. (2013). Variations of pupil centration and their effects on video eye tracking. *Ophthalmic and Physiological Optics, 33*, 634–641.